Cancer Gene Therapy (2004) 11, 333–345

www.nature.com/cgt

Herpes simplex virus thymidine kinase/ganciclovir system in multicellular tumor spheroids

Liliana ME Finocchiaro,[1,a] Viviana F Bumaschny,[1] Armando L Karara,[1] Gabriel L Fiszman,[1] Cecilia C Casais,[1] and Gerardo C Glikin[1,a]

[1]Unidad de Transferencia Genética, Instituto de Oncología "Ángel H. Roffo", Universidad de Buenos Aires, Buenos Aires, Argentina.

We have developed multicellular spheroids (MCS) established from LM05e and LM3 spontaneous Balb/c-murine mammary adenocarcinoma and B16 C57-murine melanoma derived cell lines as an *in vitro* model to study the efficacy of the herpes simplex virus thymidine kinase/ganciclovir (HSV*tk*/GCV) suicide system. We demonstrated for the first time that HSV*tk*-expressing cells assembled as MCS manifested a GCV resistance phenotype compared to the same cells grown as sparse monolayers. HSV*tk*-expressing LM05e, LM3 and B16 spheroids were 16-, three- and nine-fold less sensitive to GCV than their respective monolayers, even though they could express transgenes 10-, eight- and five-fold more efficiently. Mixed populations of HSV*tk*− and their respective βgal-expressing cells displayed a cell-type specific bystander effect that was higher in monolayers than in MCS. However, HSV*tk*−expressing cells in two- or three-dimensional cultures were always significantly more sensitive to GCV than the βgal-expressing counterparts, supporting the feasibility of this suicide approach *in vivo*. We present evidence showing that HSV*tk*-expressing tumor cells, when transferred from monolayers to MCS, displayed: (i) lower GCV cytotoxic activity and bystander effect; (ii) higher and efficient expression of genes transferred as lipoplexes; (iii) lower cell proliferation rates; and (iv) changes in intracellular Bax/Bcl-xL rheostat of mitochondria-mediated apoptosis.
Cancer Gene Therapy (2004) **11,** 333–345. doi:10.1038/sj.cgt.7700682
Published online 9 April 2004

Keywords: suicide gene therapy; lipofection; murine adenocarcinoma

Antitumor suicide gene therapy is one of the emerging strategies against cancer.[1] It consists of the introduction into cancer cells of a gene, whose product is capable of converting a nontoxic prodrug into a cytotoxic drug.[2] One of such suicide genes, the thymidine kinase gene from the herpes simplex virus (HSV*tk*), in combination with the prodrug ganciclovir (GCV), has been extensively and successfully used for the treatment of a variety of cancers in some animal models. HSV*tk* can efficiently phosphorylate the guanosine analogue GCV and allows its further transformation, after subsequent phosphorylation by cellular kinases, into cytotoxic ganciclovir-triphosphate, which inhibits cellular DNA polymerases.[3] GCV-induced apoptosis is due to incorporation of the drug into DNA resulting in replication-dependent formation of DNA double-strand breaks and, at later stages, S and G_2/M arrest.[4] As this therapeutic gene cannot be easily introduced into the whole cell population of a tumor, the successful eradication of tumors depends on a phenomenon called the bystander effect, by which the unmodified adjacent tumor cells are also sensitive to the GCV cytotoxic effect.[5,6] This bystander effect permits that the transfection of only a minority of tumor cells may lead to effective tumor regression.[6]

Despite extensive preclinical evaluation both *in vitro* and *in vivo* in several experimental models, no studies have been undertaken examining a nonviral HSV*tk*/GCV suicide system in spheroids, a model that mimics the microregions of solid tumors.[7] Multicellular spheroids (MCS) have been used as experimental models to better reflect the cellular environment that is found *in vivo*.[7–9] Being highly complex systems, their cellular properties are dependent on the origin of the tumor cells, their transformation state, medium and growth conditions.[7–9] They resemble an *in vitro* system of intermediate complexity between monolayer cultures *in vitro* and tumors *in vivo*.[7–9] In brief, MCS combine the relevance of organized tissues with the controlled environment of *in vitro* methodology.[7–9]

We have developed MCS established from M3 and M05 spontaneous Balb/c murine mammary adenocarcinomas[10,11] and the well-established murine B16 melanoma as models to explore the performance of a nonviral HSV*tk*/GCV suicide system. In this work, we present evidence showing that HSV*tk*-transfected tumor cells, when transferred from monolayer to three-dimensional

Received June 18, 2003.
Address correspondence and reprint requests to: Dr Liliana ME Finocchiaro, Unidad de Transferencia Genética, Instituto de Oncología "Dr AH Roffo" — UBA, Av. San Martín 5481, 1407 Buenos Aires, Argentina. E-mail: gglikin@bg.fcen.uba.ar
[a]On leave of absence from INGEBI-CONICET/FCEN-UBA.

culture, display: (i) lower GCV cytotoxic activity and bystander effect; (ii) higher and efficient expression of genes transferred as lipoplexes; (iii) lower cell proliferation rates; and (iv) changes in the intracellular Bax/Bcl-xL rheostat of mitochondria-mediated apoptosis.

Materials and methods

New murine cell line derived from a spontaneous mammary adenocarcinoma

Primary cultured cells, derived from M05 murine mammary adenocarcinoma were obtained, cultured, assayed for viability and stored as described.[11] Cultured as monolayers, LM05 murine adenocarcinoma was composed by two cell subpopulations: one fusiform (like fibroblasts) and the other more isometric (like epithelial cells).[11] These epithelioid cells were cloned by limit dilution, getting four identical cytokeratin-expressing clones. A pool of these four clones constituted the LM05e polyclon.

Cell cultures

Cell lines derived from M05 (LM05e), M3(LM3) and M38 (LM38) spontaneous Balb/c murine mammary adenocarcinomas;[10,11] P07 (LP07) spontaneous Balb/c murine lung adenocarcinoma;[11,12] B16-F10 (C57 murine melanoma; ATCC #CRL-6475); HeLa (human cervical adenocarcinoma; ATCC #CCL-2) and HEp-2 (human laryngeal squamous carcinoma; ATCC #CCL-23) were cultured at 37°C in a humidified atmosphere of 95% air and 5% CO_2 with IMDM/F12 medium (Hyclone, Logan, UT) containing 10% FBS (Invitrogen, Carlsbad, CA), 10 mM HEPES (pH 7.4) and antibiotics. Serial passages were performed by trypsinization (0.25% trypsin and 0.02% EDTA in PBS) of subconfluent monolayers.

MCS were prepared by using the liquid overlay technique as previously described.[7–9,13–15] Briefly, agar was diluted to 1% with serum-free medium and coated into each well preventing cell adhesion. Tumor cells (2×10^5/ml for LM3 and LM05-e or 1×10^5/ml for B16) were then plated on top of the solidified agar.

Spheroid growth

The size of sparse-growing MCS was estimated during a period of 10 days using a Neubauer camera and an inverted phase microscope. The average diameter of MCS was recorded as a measure of two diameters. The results were expressed as mean (of a minimum of 15 spheroids diameters) $\pm$ SEM (*n*: 4 independent assays).

Plasmids

$pCMV_0$ was obtained from pCMVβ[16] removing βgal gene by *Not* I digestion followed by Klenow DNA polymerase fill in and T4 DNA ligase recircularization. A *Pvu* II fragment containing HSV*tk* gene was cloned downstream of the CMV promoter after suitable adaptation in the *Not* I site of $pCMV_0$, obtaining pCMV*tk*.

Plasmids were amplified in *Escherichia coli* DH5α (Invitrogen), grown in LB medium containing 100 μg/ml ampicillin and purified using an ion-exchange chromatographic method (Qiagen, Valencia, CA).

Liposome preparation and in vitro *lipofection*

DMRIE (1,2-dimyristyl oxypropyl-3-dimethyl-hydroxyethilammonium bromide) was synthesized and provided by BioSidus S.A. (Buenos Aires, Argentina). DOPE (1,2-dioleoyl-sn-glycero-3-phosphatidyl ethanolamine) was purchased from Sigma (St. Louis, MO). Liposomes were prepared at DMRIE:DOPE molar ratios of 1:1 by sonication.[17] Cells were transfected with 1:6 μg DNA:nmol lipid in OptiMEM (Invitrogen, Carlsbad, CA). Lipoplexes (0.5 μg DNA/cm^2) were applied to cultured cells at a density of 3×10^4 cells/cm^2 (about 30% confluence). After 6–12 hours, lipofected cells were trypsinized, seeded on top of the solidified agar to form spheroids or on regular plates to form monolayers, and incubated in regular culture conditions. At the times indicated in the figures, cells were tested either for βgal expression or for their sensitivity to GCV.

β-Galactosidase assays

Assay of β-galactosidase (βgal) activity with orthonitrophenyl 1-β-D galactopyranoside (ONPG, Sigma) and *E. coli* β-galactosidase (ICN, Costa Mesa, CA) and staining of βgal-positive cells with 5-bromo-4-chloro-3-indolyl β-D-galactopyranoside (X-GAL, Sigma) were performed by standard methods.[18] To measure the efficiency of βgal gene delivery, cells were trypsinized, fixed in suspension, stained with X-GAL and counted. The βgal-stained MCS were fixed in 4% formaldehyde solution (pH = 7.4) and photographed in suspension using an inverted phase microscope.

Sensitivity to GCV assays

To test GCV cytotoxicity, 5×10^3 cells (monolayers) or 2×10^4 (MCS) of both transiently HSV*tk*- or βgal-expressing cells were incubated in 100 μl medium with 10% FBS on 96-well plates. At 24 hours after cell transfection, the medium was removed from each well and replaced with medium containing from 0.01 to 1000 μg/ml GCV (synthesized and provided by BioSidus S.A.). After 5 days, cell viability was quantified using a colorimetric CellTiter 96® Aqueous Nonradioactive MTS Cell Proliferation Assay (Promega, Madison, WI). The tetrazolium salt MTS, 3-(4,5-dimethylthiazol-2-yl)-5-(3-carboxy-methoxy-phenyl)-2-(4-sulfophenyl)-2H-tetrazolium, is converted by dehydrogenases in metabolically active cells to a formazan dye, whose absorbance at 490 nm is assumed to be proportional to the number of viable cells. The assays (where each experimental condition was performed by triplicate) were performed according to the manufacturer's instructions. The percentage of cell survival was calculated from the ratio of the absorbances between cells incubated in the presence and in the absence of GCV. The cell sensitivity to GCV,

expressed as the concentration of GCV that inhibited cell survival by 50 % (IC_{50}), was estimated from dose–response curves.

Bystander effect assays

Transiently pCMV*tk*-lipofected LM05e, LM3 and B16 cells were mixed with their respective pCMVβ lipofected controls at proportions of 0, 25, 50, 75 and 100 %. The mixtures were seeded as monolayer cultures on 96-well plates at the concentrations (cell/ml): 2.5×10^4, 5×10^4 and 1×10^5, representing the following cell densities (cell/cm^2): 10^4, 2×10^4 and 4×10^4 as indicated in the figures. Cells for MCS were seeded at 2×10^5 cells/ml (8×10^5 cells/cm^2). GCV was added and the assay proceeded as described above in the previous section.

Bromodeoxyuridine (BrdU) and connexin-43 (Cx43) immunohistochemistry

For BrdU incorporation, 1 or 4 days old MCS were incubated for 4 or 1 days, respectively, in medium agar containing 40 μM BrdU, 5 μM uridine and 0.4 μM 5-fluorodeoxyuridine as previously described.[19] At the end of the incorporation period, the medium was removed, and MCS were washed twice in PBS and resuspended in Bouin for 20 minutes. After washing three times for 5 minutes each in PBS, the pellet was resuspended in 2% liquid low-melting point agar in PBS, dehydrated in ethanol, embedded in paraffin and sectioned. Cross-sections (5 μm) of spheroids were either stained with hematoxylin and eosin or tested for BrdU or Cx43. After labeling, the slides were dehydrated through ethanol, cleared in xylol and coverslip was affixed.

For BrdU labeling, cross-sections of MCS were rehydrated and rinsed in PBS several times, incubated 15 minutes in 0.1 N HCl/Triton X-100 and digested by the endonuclease/exonuclease procedure to create single-stranded regions in the DNA to expose the incorporated BrdU to antibody.[19,20] Sections were then treated with 1 M Tris-HCl (pH = 7.5) to block the formaldehyde; with 0.2% Triton X-100 in PBS and finally with H_2O_2 to block endogenous peroxidase activity prior to the application of the primary antibodies in PBS containing 0.5 mg/ml BSA and 0.05% Triton X-100.

Immunohistochemistry was performed by standard procedures using the specific polyclonal anti-Cx43 or the monoclonal anti-BrdU antibodies as the first antibody at 5 and 12.5 μg/ml, respectively. For the immunocytochemical detection, the corresponding biotin-labeled second antibody was used according to the host in which the primary antibody was raised. The immunoreactive product was visualized with a substrate solution of 3,3′-diaminobenzidine and H_2O_2. Monoclonal antibody against BrdU was a kind gift from Dr T Ternynck (Institut Pasteur, Paris, France). The specific rabbit polyclonal anti-Cx43 antibody corresponding to a segment of the third cytoplasmic domain was from Zymed (San Francisco, CA).

DNA synthesis determinations

DNA synthesis was evaluated after 24 hours of incubation of LM3, LM05e and B16 cells multiwell plated as either monolayers or MCS by ^{3}H-thymidine (New England Nuclear, Boston, MA; 1.2 Ci/mmol) incorporation as described earlier.[19] ^{3}H-thymidine (0.1 μCi/well; 1.2 Ci/mmol) was added to the cultures and incubation lasted for 1 and 5 days. At the times indicated in the figures, cells were harvested on glass fiber filters with a multiwell cell harvester (Nunc, Rochester, NY). Radioactivity was measured in a β-scintillation counter.

Western blot analysis

Cells from two (2D)- or three-dimensional (3D) cultures were harvested, rinsed with PBS and stored as cell pellets at –70°C until ready for use. Cell lysates (25 μg protein in ice cold NP-40 lysis buffer), sonicated and clarified by centrifugation, were resolved by SDS-polyacrylamide gel electrophoresis, blotted onto Immobilon-P membranes (Millipore, Bedford, MA). The filter was incubated in a solution of 50 mM Tris-HCl (pH = 7.5), 150 mM NaCl, 0.05% Tween-20, 5% dried low fat milk for 12 hours and then probed with rabbit polyclonal anti-Cx43 antibody (described above), mouse monoclonal anti-Bax, or anti-Bcl-xL (BD Biosciences, Lexington, KY), or anti-actin antibodies (Sigma) at a concentration of 2, 0.25, 0.25 and 1.5 μg/ml in TBS-T. Horseradish peroxidase-conjugated goat antimouse IgG (Sigma) was used as second antibody (1:1000 dilution) for 1 hour. Protein bands were detected by ECL Detection System (Amersham, Uppsala, Sweden) according to the manufacturer's instructions.

Protein determinations

Protein concentrations were determined by the Bradford method.[21]

Statistical analysis

Results were expressed as means ± standard error of the mean (SEM) (*n*: number of experiments corresponding to independent assays). Statistics were determined by analysis of variance (ANOVA).

Results and Discussion

Tumor cells grew in vitro *as multicellular spheroids*

Multicellular spheroids (MCS) represent a highly valuable *in vitro* tumor model to explore the efficacy of the HSV*tk*/GCV suicide gene therapy system, under conditions that more closely resemble the *in vivo* situation.[8,9]

Although some tumor-derived cell lines, like LP07 (murine lung adenocarcinoma),[11,12] were not able to grow *in vitro* as spheroids, LM3, LM05e and LM38 (murine mammary adenocarcinomas),[10,11] B16 (murine melanoma), HeLa (human cervical adenocarcinoma) and HEp-2 (human laryngeal squamous carcinoma), readily formed MCS when plated on top of solidified agar (data not shown). While LM05e and LM3 spheroid cells appeared

intimately associated with each other and closely packed, B16, LM38, HeLa and HEp-2 formed more loosely associated aggregates of cells in which single cells could be clearly distinguished (data not shown). We focused our study on LM05e, LM3 and B16 tumor-derived cell lines that in preliminary experiments displayed differential behavior with respect to the HSV*tk*/GCV system.

Spheroids were more resistant than their respective monolayers to the HSVtk/GCV system

As far as we know, we explored for the first time how the spatial configuration of cells could affect the efficacy of the HSV*tk*/GCV system. The cytotoxicity of increasing concentrations (0.1–1000 μg/ml) of the prodrug GCV was tested on monolayers and MCS of HSV*tk*-expressing LM05e, LM3 and B16 cells (LM05e/*tk*, LM3/*tk* and B16/*tk*). The same cells transiently expressing βgal gene (LM05e/β, LM3/β and B16/β) were used as negative controls.

All the HSV*tk*-transfected cell lines manifested a relative GCV resistance phenotype when grown as MCS, compared to the same cells grown as sparse monolayer cultures. HSV*tk*-expressing LM05e, LM3 and B16 spheroids were about 16-, three- and nine-fold less sensitive to GCV than the same cells in monolayers (Fig 1 and Table 1). However, in every assay performed in 2D or 3D cultures, all the HSV*tk*-transfected cells were significantly more sensitive to GCV than the respective βgal-transfected controls, as derived from IC_{50} data

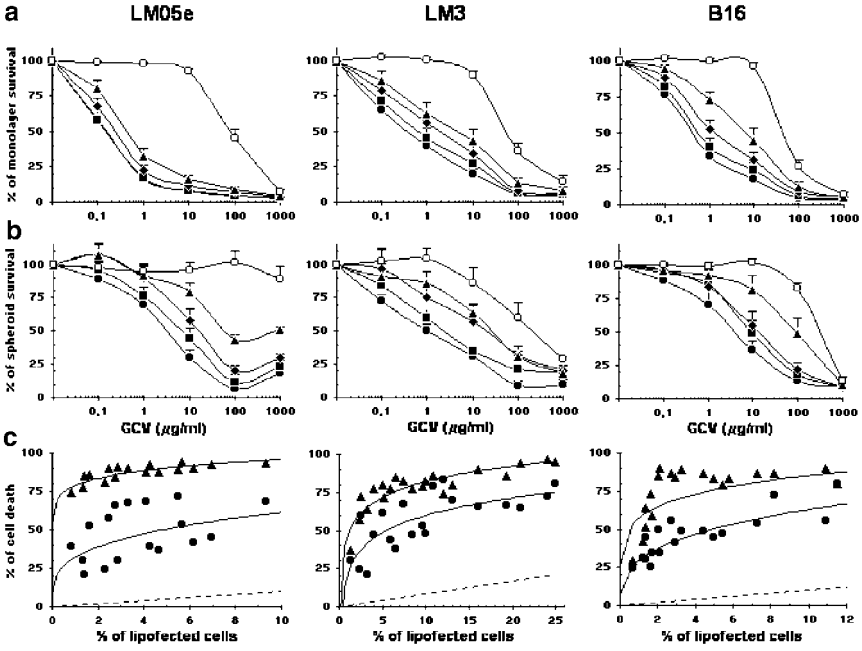

Figure 1 *In vitro* bystander effect in monolayers and spheroids. (**a**) and (**b**) *In vitro* GCV sensitivity of different combinations of LM05e, LM3 and B16 HSV*tk*-and βgal-expressing cells. GCV dose–response curves of cells growing as monolayers (**a**) or spheroids (**b**). The assay was performed as described in Materials and methods. Results are expressed as mean$\pm$standard error of the mean (sem) of five (LM05e), seven (LM3) and six (B16) independent experiments. Ratios of HSVtk/βgal-expressing cells: 100/0 (●); 75/25 (■); 50/50 (♦); 25/75 (▲); 0/100 (○). (**c**) Proportion of surviving cells as a function of the number of HSV*tk*-expressing cells at a fixed 10 μg/ml GCV concentration. Values of individual experiments, where each experimental condition was performed in triplicate, are plotted. Spheroids (●); monolayers (▲). The dotted line represents the expected theoretical curve if there was no bystander effect.

Showing the *P*-values obtained by ANOVA test statistical analysis performed for 10 μg/ml GCV concentration. $P<.05$ in bold.

HSVtk/βgal	LM05e	LM05e	LM3	LM3	B16	B16
(a)	HSVtk vs.	βgal I vs.	HSVtk vs.	βgal vs.	HSVtk vs.	βgal vs.
75/25	0.73	**9.5E-10**	0.25	**1.8E-07**	0.37	**4.6E-07**
50/50	0.11	**3.1E-09**	**0.04**	**1.5E-06**	0.06	**7.7E-07**
25/75	**0.01**	**1.7E-08**	**0.01**	**5.7E-05**	**0.02**	**0.0002**
0/100	**7.2E-10**		**1.2E-09**		**1.8E-08**	
(b)						
75/25	0.18	**0.001**	0.58	**0.005**	0.32	**0.0002**
50/50	**0.028**	**0.008**	0.07	0.12	0.19	**0.002**
25/75	**0.0007**	0.12	**0.004**	0.14	**0.006**	0.07
0/100	**4.9E-05**		**0.001**		**4.3E-06**	

Table 1 *In vitro* sensitivity to GCV of HSV*tk*- and βgal-expressing multicellular spheroids (MCS) or monolayer cultures (MLC)

			Monolayer cultures			Multicellular spheroids			
Cell line	*n*	Lipofection efficiency (%)	IC_{50} βgal (μg/ml GCV)	IC_{50} TK (μg/ml GCV)	IC_{50} βgal/ IC_{50} TK	IC_{50} βgal (μg/ml GCV)	IC_{50} TK (μg/ml GCV)	IC_{50} βgal/ IC_{50} TK	IC_{50} TK MCS/IC_{50} TK MLC
LM05e	5	6.0±1.1	96±23	0.18±0.06*	533	>1000	2.8±0.9*/#	357	16
LM3	7	16.8±3.5	91±28	1.0±0.4*	91	358±181	3.3±1.4	108	3
B16	6	9.2±3.7	49±7	0.7±0.3*	70	290±21	6.0±3.0*	48	9

Lipofection efficiency was measured as X-Gal blue-stained cells. The results represent means±SEM of GCV concentrations leading to a 50% reduction in cell viability (IC_{50}) from the experiments showed in Figure 1. Differences between groups were determined by analysis of variance (ANOVA). *n* = number of experiments corresponding to independent assays; *$P<.05$ = the IC_{50} for GCV of *HSVtk* vs. βgal-expressing cells. #$P<.05$ = the IC_{50} for GCV of *HSVtk*-expressing cells in spheroids vs. monolayers.

(Fig 1a and b; Table 1). This fact supports the feasibility of this suicide approach *in vivo*.

Assembled as MCS, βgal-expressing cells were less sensitive to GCV than grown as monolayer cultures. In the case of LM05e 3D-cultures, the pCMVβ-transfected cell-survival curve was greatly retarded, impairing the interpolation of the corresponding IC_{50}, and consequently, comparative results became less accurate. This lack of sensitivity to GCV could be overcome by a long-term exposure to this prodrug. After 10 days, βgal-expressing LM05e spheroids displayed an IC_{50} of about 200 μg/ml GCV, while HSV*tk*-expressing LM05e IC_{50} did not significantly change.

The in vitro *bystander effect was modulated by cell spatial configuration*

To determine the extent of the *in vitro* bystander effect, various proportions (100/0, 75/25, 50/50, 25/75, 0/100) of pCMV*tk*/pCMVβ-lipofected LM05e, LM3 and B16 cells were 2D and 3D cocultured for 5 days with increasing concentrations (0.1–1000 μg/ml) of GCV. As shown in Figure 1a, HSV*tk*-expressing LM05e monolayer cultures were the most sensitive to increasing concentrations of GCV. Dilution with arising amounts of βgal-expressing LM05e cells had little effect on GCV sensitivity in this particular adenocarcinoma cell line. Cell-survival curves of 25 and 50% LM05e/*tk* cells were similar to those of 75 and 100% LM05e/*tk* cells, suggesting a strong bystander effect. In the case of LM3 and B16 monolayers, cells became more sensitive to dilution with their respective βgal-expressing cells, suggesting a lower bystander effect (Fig 1a). When transferred from 2D- to 3D-cultures, LM05e, LM3 and B16, cell-survival curves readily shifted rightward as the percentage of HSV*tk*-expressing cells decreased, suggesting a weaker bystander effect in MCS (Fig 1b).

The bystander effect becomes evident when GCV-induced cell killing is not restricted to the cells that express the suicide gene.[5,6] Figure 1c shows the proportion of cell death at 10 μg/ml GCV, with respect to the fraction of cells that expressed the transfected gene (percentages of HSV*tk*-lipofected cells corrected for their respective transfection efficiency, measured as a percentage of βgal-expressing cells). We estimated the bystander effect at the pharmacologically relevant GCV concentration of 10 μg/ml (comparable to a standard dose for human patients), which killed most of HSV*tk*-expressing cells, with little effect on βgal-expressing cells (Fig 1 a and b). The dotted line represents the theoretical percent of cell death if there was no the bystander effect. All the curves were above this theoretical line, indicating the presence of the bystander effect for the three tested cell lines, regardless of their culture spatial configuration. Only 1% LM05e/*tk* cells was sufficient to induce a powerful bystander effect that killed 80 and 30% of the 2D- and 3D-cultured cells, respectively (Fig 1c). The presence of 5% LM05e/*tk* cells was enough to destroy, respectively, 90 and 50% of the 2D- and 3D-cultures (Fig 1c). This effect was lower for LM3/*tk* or B16/*tk* cells, where at 5% proportion, they were able to destroy, respectively, 70 and 45% or 75 and 50% of the 2D- and 3D-cultures (Fig 1c). It is worth noting that MCS displayed similar sensitivity to 10 μg/ml GCV in the three cell lines tested, regardless of their different behavior in monolayer.

The bystander effect was modulated by cellular physical contact and the proliferative state in monolayers

The potency of the bystander effect associated with the HSV*tk*/GCV system is supposed to be upregulated by physical contact among cells.[22] Three-dimensional organization of cancer cells as MCS is based upon cells in close proximity to one another with a higher number of cell-to-cell interactions than monolayer cultures.[23] Then, it seemed logical to expect a higher bystander effect in MCS with respect to monolayer cultures. However, the 3D-geometry not only did not increase but also significantly diminished the bystander effect (Fig 1).

To address this issue in greater detail, we compared the GCV cell-survival curves in monolayers seeded at three different cell densities: 2.5×10^4, 5×10^4 and 1×10^5 cells/ml (8.5×10^3, 1.7×10^4 and 3.5×10^4 cells/cm^2). In this way, we obtained cultures with a varying degree of cell-to-cell contacts.

Figure 2 shows that, when βgal-expressing LM05e, LM3 and B16 monolayer cells were cocultured with their respective HSV*tk*-expressing counterparts, at the intermediate density in which most cells were contacting one another, they were markedly eliminated by 10 μg/ml GCV. Conversely, when cocultured at low cell density, a weaker but significant bystander effect was observed. Furthermore, media conditioned by HSV*tk*-expressing LM05e, LM3 and B16 monolayer cells treated with GCV exhibited a weak cytotoxic effect on the parental cells (data not shown). These results indicate that the bystander effect could require close proximity or direct contact between HSV*tk*-expressing cells and neighbor cells and that some cytotoxic molecules released from HSV*tk*-transfected cells could be minor contributors to this phenomenon.

It is noteworthy that the GCV cell-survival curves of HSV*tk*-expressing cells growing at high-density cultures, with high degree of cell–cell contacts, did not improve the bystander effect. The effectiveness of cell cycle-dependent HSV*tk*-based suicide gene therapy system could be limited by a decrease of the proliferating cell fraction at high densities as was confirmed by ^{3}H-thymidine incorporation into DNA. As shown in Figure 3a, the initial levels of monolayer ^{3}H-thymidine incorporation were proportional to the number of cells seeded, being higher in

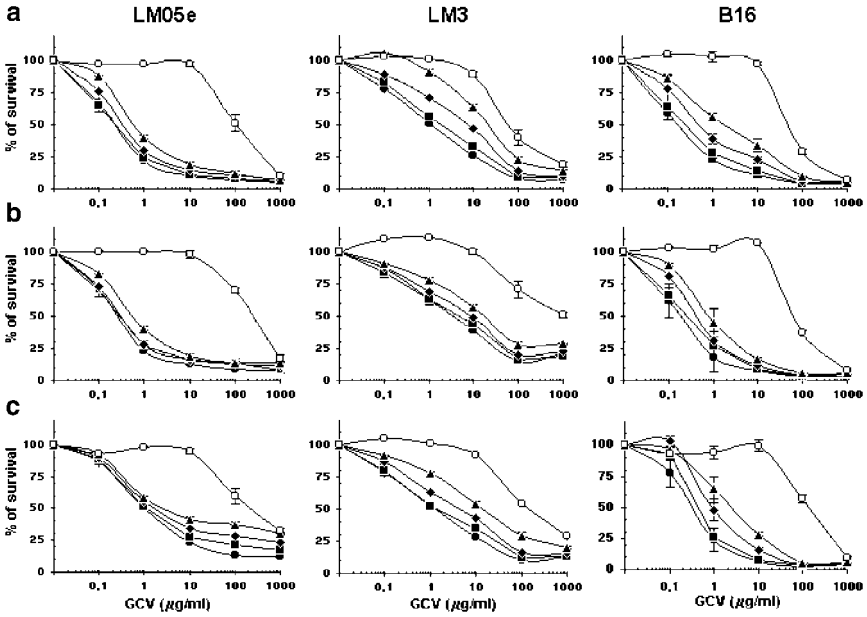

Figure 2 Effect of monolayer cell density on GCV sensitivity. *In vitro* GCV sensitivity of different combinations of LM05e, LM3 and B16 HSV*tk*- and βgal-expressing cells. GCV dose–response curves of cells growing as monolayers seeded at different cell densities (cell/cm^2): 10^4 (**a**), 2×10^4 (**b**) and 4×10^4 (**c**). The assay was performed as described in Materials and methods. Results are expressed as mean ± SEM of four independent experiments. Ratios of HSVtk/βgal-expressing cells: 100/0 (●); 75/25 (■); 50/50 (♦); 25/75 (▲); 0/100 (○).

Showing the *P*-values obtained by ANOVA test statistical analysis performed for 10 μg/ml GCV concentration. $P < .05$ in bold.

HSVtk/βgal	LM05e	LM05e	LM3	LM3	B16	B16
(a)	HSVtk vs.	βgal I vs.	HSVtk vs.	βgal vs.	HSVtk vs.	βgal vs
75/25	0.68	**1.8E-08**	**0.005**	**0.0001**	0.23	**2.4E-08**
50/50	**0.002**	**1.0E-08**	**5.1E-05**	**0.0007**	**0.02**	**5.8E-07**
25/75	**0.001**	**3.3E-08**	**0.004**	**0.054**	**0.006**	**2.6E-05**
0/100	**4E-09**		**6.7E-05**		**4.3E-08**	
(b)						
75/25	0.21	**1.6E-07**	0.24	**4.8E-05**	0.73	**5.6E-11**
50/50	0.33	**7.0E-07**	0.06	**0.0002**	0.15	**4.9E-13**
25/75	0.07	**4.3E-07**	**0.01**	**0.002**	**0.001**	**2.8E-10**
0/100	**2E-07**		**1.9E-05**		**4.5E-09**	
(c)						
75/25	0.76	**0.002**	0.65	**0.0007**	**0.06**	**1.2E-07**
50/50	0.38	**0.002**	0.30	**0.0009**	**0.002**	**2.1E-07**
25/75	0.17	**0.005**	**0.04**	**0.004**	**0.001**	**8.0E-07**
0/100	**0.001**		**0.0002**		**8.9E-08**	

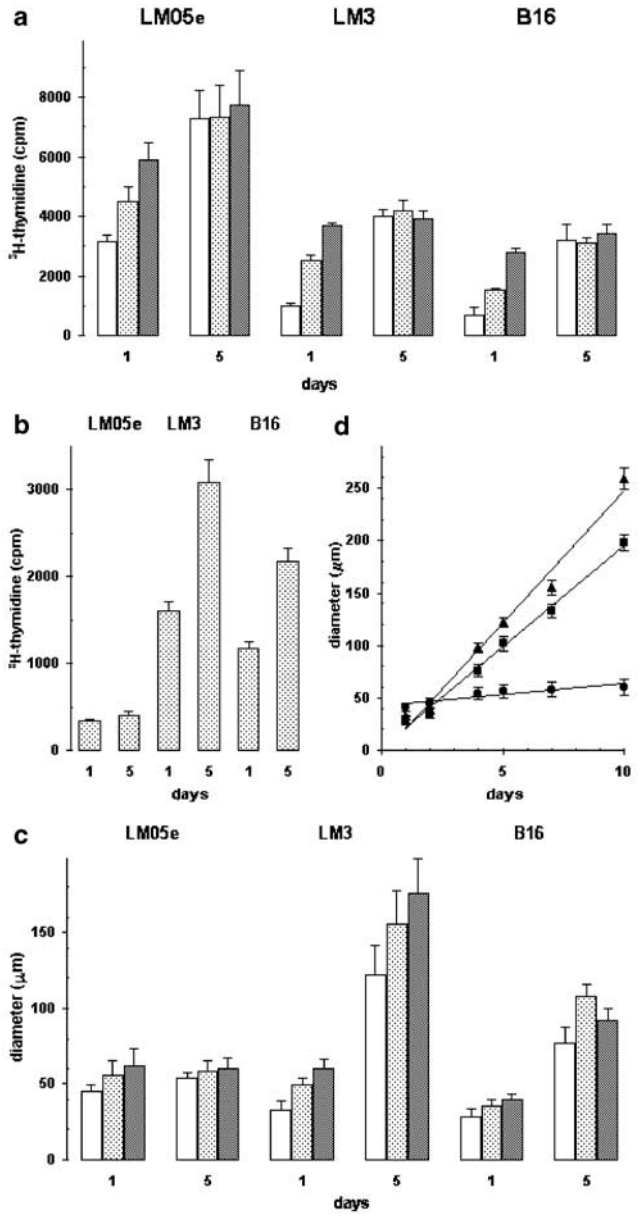

Figure 3 Cell growth parameters in monolayers and spheroids. (**a**) ^{3}H-thymidine incorporation into DNA of LM05e, LM3 and B16 monolayers seeded at different cell densities (cells/ml): 2.5×10^4 (white bars), 5×10^4 (light gray bars) and 1×10^5 (dark gray bars) as indicated. Cells were pulsed with ^{3}H-thymidine and harvested at day 1 or day 5 as described in Materials and methods. Each point represents the mean $\pm$ SEM of four determinations of the amount of ^{3}H-thymidine incorporated into DNA. (**b**) ^{3}H-thymidine incorporation into DNA of LM05e, LM3 and B16 spheroids. Cells were pulsed with ^{3}H-thymidine and harvested at day 1 or day 5 as described in Materials and methods. Each point represents the mean $\pm$ SEM of four determinations of the amount of ^{3}H-thymidine incorporated into DNA. (**c**) Spheroid size as a function of seeding cell density (cells/ml): 1×10^5 (white bars), 2×10^5 (light gray bars) and 4×10^5 (dark gray bars). The average spheroid diameters (calculated from 20 measurements) were taken after 1 day or 5 days as described in Materials and methods. (**d**) Spheroids growth curves. The average spheroid diameters (calculated from 20 measurements) were plotted as a function of time. LM05e (●); LM3 (▲); B16 (■).

LM05e than in LM3 and B16 monolayers. At day 5 every cell culture reached a plateau level regardless of the initial cell density.

Spheroids displayed a high fraction of quiescent cells

Although numerous studies utilizing cultured cells in 3D aggregates have shown that, in fact, cells grown as spheroids behave in a different manner with respect to cells in monolayers no studies have determined the mechanisms that may account for the development of GCV resistance in MCS.[7–9,13–15] It is therefore plausible to speculate that a compromised GCV access, an active drug efflux, or a low proliferating fraction in MCS, could limit the effectiveness of DNA replication-dependent HSV*tk*-based suicide gene therapy system.

MCS incorporated less ^{3}H-thymidine than an equivalent amount of the corresponding monolayer cells, LM05e spheroids being the least active (Fig 3a and b). It is worth noting the correlation between ^{3}H-thymidine incorporation into DNA and the increase in MCS diameter during the 5-day period observed in Figure 3b, d. Figure 3c shows that, even though initial spheroid diameter (day 1) was slightly proportional to the number of seeded cells, spheroid proliferating cell fraction was not limited by high cell densities as it occurred in monolayers (Fig 3a). Whereas LM05e spheroids did not display any significant size increase from day 1 to 5, LM3 and B16 significantly enlarged their diameter during the same period regardless of the initial seeding cell density.

Figure 3d reveals the different growth potentials of LM05e, LM3 and B16 spheroids. While LM3 and B16 spheroids showed extensive growth, increasing their initial diameter about eight and six times, respectively, during the first 10 days, LM05e compact spheroids showed only a slight increase of 1.2 times the initial diameter during the same period. Spheroid growth curves showed no significant differences between transfected and nontransfected cell lines (data not shown).

The bromodeoxiuridine-labeled (BrdU-) replication profiles of Figure 4 confirmed the proliferative status of tumor cells at different depths within MCS.[19,24] Long-term (5 days) BrdU incorporation into 1-day-old LM3 and B16 spheroids yielded intense BrdU nuclear staining distributed throughout the spheroid (Fig 4a-c). On the other hand, with short-lasting BrdU pulses (1 day) into 5-day-old MCS, there was a high fraction of nonproliferating or quiescent cells (Fig 4d–f). The replication active part of MCS, sensitive to the suicide system, mainly belonged to the outer layers, yielding the shrunken MCS that we found after HSV*tk*/GCV treatment (Fig 4j–o). These results suggest that in this spatial configuration, cells appear to proliferate as monolayers on the surface of a sphere. As expected, only a few stained cells were observed in the highly compacted LM05e spheroids, after 5 days of BrdU exposure. This suggests a compromised BrdU penetration and/or a higher fraction of quiescent cells that would be naturally resistant to this cell cycle-dependent HSV*tk*/GCV system. Considering that in Figure 4a-f, all the photographs have the same magnification, the

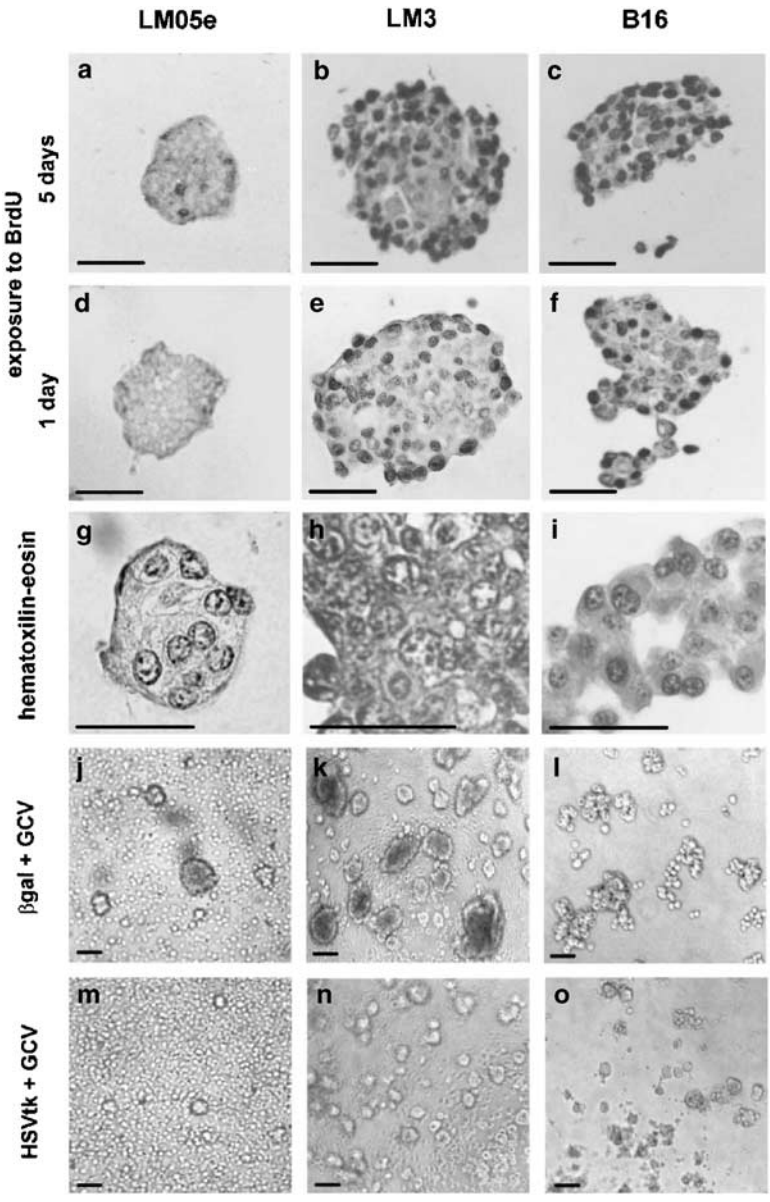

Figure 4 : BrdU incorporation in spheroids. (**a–f**) BrdU incorporation in LM05e, LM3 and B16 spheroids. Cells grown as spheroids for 1 (**a-c**) or 5 days (**d–f**) were incubated with BrdU for 5 (**a–c**) or 1 days (**d–f**) as described in Materials and methods. (**g-i**) Hematoxylin and eosin staining of 5-day-old LM05e, LM3 and B16 multicellular spheroids sections. Spheroids were collected, embedded in paraffin and cross-sections were stained for BrdU or hematoxylin and eosin as indicated in Materials and methods. (**j–o**) GCV sensitivity of LM05e, LM3 and B16 HSV*tk*-expressing spheroids. Cells grown as spheroids for 1 day were incubated in the presence or absence of 10 μg/ml GCV during 5 days as described in Materials and methods. Aliquots of spheroids suspensions were photographed using an inverted phase microscope, as described in Materials and methods. Black bars in the lower left corner represent 50 μm.

highly compacted nature of LM05e aggregates with respect of those of LM3 and B16 was easily noticed. This probably constituted a permeability barrier to GCV, as suggested by the fact that after 5 days of treatment with high GCV concentrations, 100% of LM05e/β spheroids remained metabolically active. However, after 10 days of treatment, these spheroids were as sensitive as LM05e/β monolayers after 5 days of treatment (data not shown). Then, penetration of GCV molecules from high external concentrations into deeper layers and core of MCS was dependent on exposure time and the spheroid structure characteristic of each tumor cell.

In the case of HSV*tk*-expressing cells, only GCV short-term exposure is required to initiate an irreversible event cascade, leading to programmed cell death, which occurs over several days.[6] It was reported that, once GCV entered the cells, it is readily phosphorylated by HSV*tk*, losing its ability to pass through cell membranes.[25,26] Thus, its half-life within the cell is about six-fold longer than that of unmodified GCV.[25,26] Preliminary data of

our laboratory showed that 1 or 5 days of exposure to GCV yielded similar cytotoxic activity and bystander effect on 2D- and 3D- assembled HSV*tk*-expressing cells (data not shown).

On the other hand, histological sections stained with hematoxylin and eosin demonstrated that untreated 6-day-old MCS had well-preserved cells throughout the spheroid with no visible necrotic areas (Fig 4g-i). The uniformly distributed chromatin and the evident nucleoli suggested pronounced cell activity.

Connexin-43 was expressed in monolayers and spheroids of the three cell lines tested

A modulation in the expression of the molecules that are directly responsible for cell-to-cell interactions may be involved in the extent of the HSV*tk*/GCV bystander effect.[27] Gap junctions, cellular channels built up by proteins called connexins, are of special interest because they allow the transfer of toxic GCV metabolites from HSV*tk*-transfected tumor cells to the wild-type tumor cells, thus contributing to cell death.[27,28] Most tumors and cancer cell lines have lost their ability to communicate through gap junctions.[29,30] Since in MCS, the expression of connexins is usually downregulated with respect to monolayers,[31] we investigated the expression of connexin-43 (Cx43), a major gap junction-forming connexin protein in these 2D- and 3D-cultured tumor cells. A specific polyclonal antibody directed against a Cx43 cytoplasmic domain was employed to investigate the Cx43 presence in LM05e, LM3 and B16 cells growing as monolayers and MCS by immunohistochemistry and Western blot analysis.

Figure 5a-f shows characteristic punctuate of Cx43 staining at cytosol and gap junction plaques of LM05e, LM3 and B16 monolayers. Substantially, a more diffused pattern of Cx43 labeling was observed in 3D- than in 2D-cultures, LM05e spheroids being the best immunostained.

As shown in Figure 5h, Western blot detected the higher levels of the Cx43 in 2D- (lane 3) and 3D- (lane 2) LM05e cells. Other bands appearing in the blot were non-specific, since Cx43 antibody crossreactivity with other connexins has not been observed in Western blots (as described by the manufacturer). Semiquantitative analysis of scanned blots indicated that LM05e cell spheroids expressed from five- to two-fold the amount of Cx43 with respect to LM3 or B16 spheroids. No significant differences were found between monolayers and spheroids

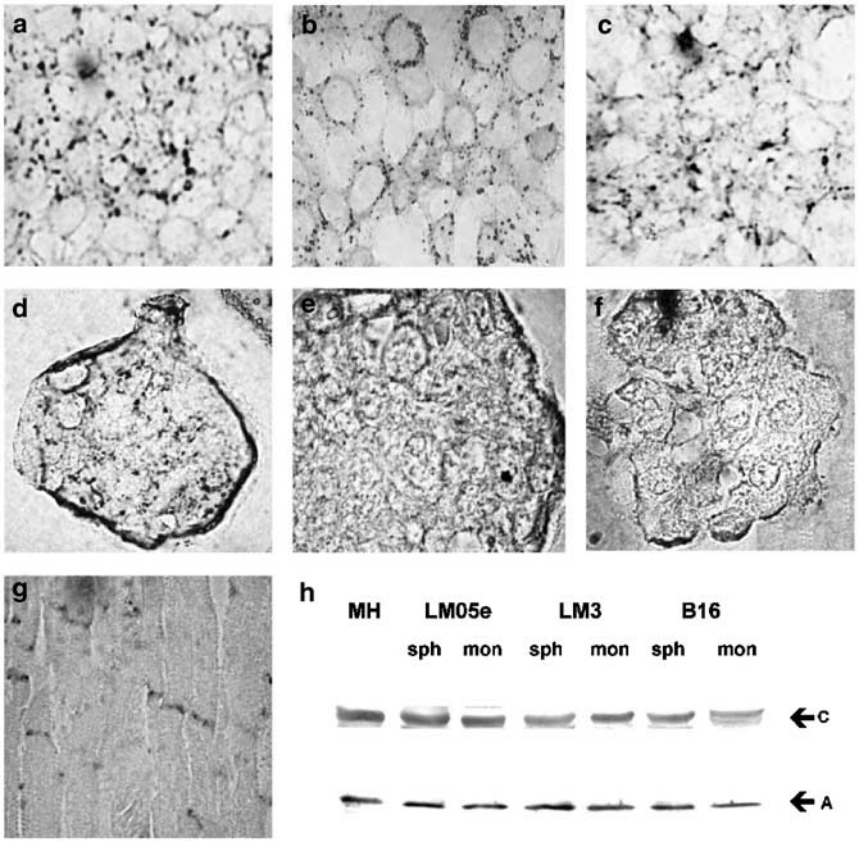

Figure 5 Connexin-43 expression in monolayers and spheroids. (**a**-**g**) Cx43 immunostaining in LM05e, LM3 and B16 cells cultured as monolayers (**a**–**c**) or spheroids (**d**–**f**) and in control mouse heart cells (**g**) performed as described in Materials and methods. (**h**) Western blot analysis of Cx43 in LM05e, LM3 and B16 cells cultured as monolayers (mon) or spheroids (sph) was performed as described in Materials and methods. Cx43 (C).migrated at 43 kDa. Constitutive actin expression controls (A). Similar results were obtained in three separate experiments.

in LM05e, but LM3 spheroids displayed one-third of Cx43 with respect to LM3 monolayers, while B16 spheroids triplicated the respective monolayer values.

Both immunostaining and Western blot indicated higher Cx43 levels in LM05e cells, a fact that correlated with the higher GCV sensitivity and bystander effect in a context of lower gene transfer efficiency and expression, and would partially explain the differences in GCV sensitivity and bystander effect in LM05e with respect to other cell lines tested.

Spheroids displayed enhanced transgene expression

Cell sensitivity of tumor spheroids to HSV*tk*/GCV would depend on the efficiency of HSV*tk* gene transfer and expression. To determine if spheroid GCV resistance was due to reduced transgene expression, the temporal course of HSV*tk* expression during GCV treatment was indirectly monitored by βgal-coexpression.

LM05e, LM3 and B16 cells were *in vitro* colipofected with pCMVβ and pCMV*tk* or pCMV$_0$ (the empty vector). After 24 hours, part of the cells was then seeded on coated plates as MCS while the other was kept in 2D-cultures. After 1–4 days incubation in medium with 1 μg/ml GCV, cells were assayed for βgal activity. The mean values varied greatly in the HSV*tk*-coexpressing group, where βgal was only coexpressed by the fraction of cells that survived to GCV exposure. Owing to this, data were expressed as βgal-specific activity (mU βgal/μg protein).

Perhaps the most surprising finding was that βgal-specific activity was considerably higher in cells grown in spheroids compared to the same cells in logarithmic growth phase monolayers, in all the assayed conditions, suggesting that 3D-configuration strongly enhanced transgene expression (Fig 6). At every cell density, culture geometry and cell cycle stage, βgal was detected. HSV*tk* by itself was totally nontoxic to cells so, in the absence of GCV, they remained 100% viable *in vitro* (data not shown). In addition, the general pattern of βgal-specific activity observed in the absence or presence of GCV was the same, showing conclusively that GCV treatment did not affect specific gene expression (data not shown). As shown in Figure 6, every cell line displayed a different expression pattern. It is worth noting that βgal-specific expression dramatically increased during the 4-day period in LM05e and LM3 spheroids, while it decreased in B16. After 4 days in monolayers, βgal expression remained constant or decreased, probably due to the decline in the percentage of transfected cells by transgene dilution during replication of the target population or loss of the transgene by nuclease destruction or partitioning to nonnuclear compartments. When transferred from monolayers to slowly proliferating spheroids, there was a strong increase of βgal-specific expression being maximal on day 4 in LM05e (10-fold) and LM3 (eight-fold) cells, and on day 1 in B16 (five-fold) (Fig 6). It is worth noting that: (i) GCV/HSV*tk*-cell-killing did not significantly affect βgal-specific expression of surviving cells over a 4-day period and, (ii) there was a diminution of βgal expression in MCS cotransfected with pCMV*tk* (carrying the gene) with

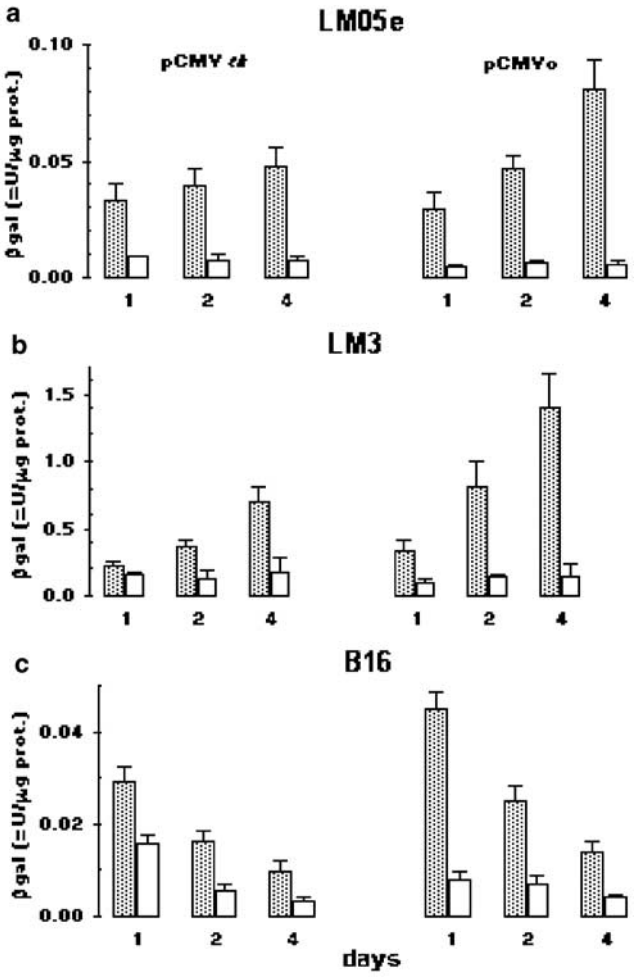

Figure 6 Transgene expression in monolayers and spheroids. Time course of βgal reporter gene expression LM05e, LM3 and B16 cell growing as monolayers (white bars) and spheroids (gray bars). Cultured cells were *in vitro* colipofected with pCMVβ and pCMV*tk* or pCMV$_0$ as indicated. After 24 hours, part of the cells was then seeded on coated plates as multicellular spheroids, while the others were kept as monolayers. After 1, 2 and 4 days of incubation in regular culture conditions with or without 10 μg/ml GCV, cells were homogenized and assayed for βgal activity as described in Materials and methods. Results are expressed as mU of βgal activity/μg protein $\pm$ SEM of four determinations after correction for background.

respect to pCMV$_0$ (empty plasmid), even in the absence of GCV (data not shown). This effect confirmed the high coexpression levels of this suicide gene that was employing an important fraction of the spheroid cellular machinery involved in gene expression. In general terms, spheroid maximal transgene expression was, respectively, about 20- and 40-fold higher in LM3 with respect to LM05e and B16. These data also indicate that the tumor type would not determine its GCV sensitivity or its ability to express foreign genes. Between two spontaneous mammary adenocarcinoma cells, LM05e, with a relatively low gene transfer and expression, was five-fold more sensitive to GCV (IC_{50}s: 0.18 ± 0.05 *vs* 1.0 ± 0.3 μg/ml) in monolayers and as sensitive (IC_{50}s: 3.3 ± 2.4 *vs*

$2.8 \pm 0.7\ \mu$g/ml) in spheroids as LM3, which showed a fairly high lipofection efficiency and transgene expression (Table 1).

The effects of spatial configuration on βgal reporter gene expression were confirmed by X-GAL staining of βgal-lipofected cells. Figure 7 shows representative micrographs of X-GAL-stained LM05e, LM3, and B16 cells seeded 24 hours after pCMVβ lipofection as MCS. It is noteworthy that the βgal gene expression, clustered in defined regions throughout the spheroid, increased in LM05e and LM3 spheroids from day 1 to 5 (2–6 days after lipofection), while it decreased in B16. The correlation between βgal and HSVtk coexpression was indirectly confirmed by colipofection of LM05e, LM3 and B16 with pCMVβ and a plasmid carrying the coding gene for mouse interleukin-4 (mrIL-4). As measured by ELISA assay, 7 days after lipofection, secreted mrIL-4 was, respectively, eight-, seven- and four-fold higher in 3D- with respect to 2D-cultures (the spheroids and monolayers LM05e, LM3 and B16 production being: 46.8 ± 5.1/5.7 ± 1.1; 220 ± 44/32 ± 3.78; 1.47 ± 0.82/0.29 ± 0.08 ng mrIL-4/μg protein/day respectively (these results are expressed as means $\pm$ SEM of three independent experiments). Our data do not agree with those of Klunder and Hulser,[14] which found a reduced portion of producing cells in MCS, relative to the same cells grown in monolayers. Since their transgene expression was regulated by β-actin promoter, this apparent contradiction could be explained by the differences in the levels of regulatory factors that bind to β-actin or CMV promoters in 2D- and 3D-cultured cells.

This set of data suggests that in all the assayed conditions, cells growing as MCS expressed significantly higher transgene levels than the same cells grown in monolayers, suggesting that 3D-configuration profoundly affected gene expression. These findings discarded the assumption that an increase in the number of transfected cells (Table 1) or the amount of recombinant enzyme synthesized (as derived from Figures 6 and 7) would be enough to improve either its sensitivity to GCV or the bystander effect (Fig 1). Furthermore, this fact supports the possible use of lipoplexes as vectors for this suicide approach *in vivo*.

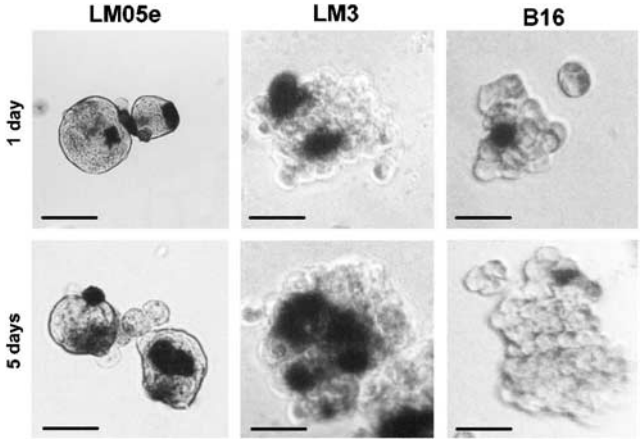

Figure 7 βgal expression in spheroids. LM05e, LM3 and B16 cells were transfected *in vitro* with lipoplex containing pCMVβ, harvested 24 hours later and seeded on coated 35 mm plates as multicellular spheroids. Specimens were fixed in suspension and stained with X-Gal 2 and 5 days later, as described in Materials and methods. Similar results were obtained in seven separate experiments. Black bars in the lower left corner represent 50 μm.

Apoptosis mediators were differentially regulated in monolayers and spheroids

As shown in Figure 8, there was a significant correlation between HSV*tk*/GCV-induced killing and changes of intracellular proapoptotic/antiapoptotic proteins such as Bax/Bcl-xL, investigated by Western blot analysis. Increased Bax and decreased Bcl-xL levels after GCV treatment support the higher sensitivity to GCV of LM05e/*tk* and B16/*tk* monolayers with respect to their respective spheroids, where GCV increased both Bax and Bcl-xL (3D-LM05e) or did not modify them (3D-B16).[4,32,33] In the case of LM3, a similar GCV-induced Bax increase, without changes in Bcl-xL levels, could explain the similar GCV sensitivity and the bystander effect of 2D- and 3D-LM3 cultures.[4,32,33]

Additional factor(s) should be involved in the bystander effect of nonreplicating spheroid cells

Although considerably high transgene expression by itself could account for the efficacy of the HSV*tk*/GCV suicide system in LM3 spheroids, the situation was different for the other cell lines tested. When seeded at high density, increasing cell- to- cell contacts, LM05e and B16 monolayers diminished their growth rates, GCV sensitivity and bystander effect, behaving as slow growing LM05e spheroids (Figs 1-3). In this case, B16 spheroids were proliferating at a rate comparable to that of LM3 spheroids but displaying higher connexin-43 expression level (Fig 5h) and lower transgene expression (Fig 6). Then, these expression patterns could partially produce the observed differences in cell sensitivity to GCV and the bystander effect. Both LM3 and LM05e spheroids significantly increased their βgal-specific activity as long

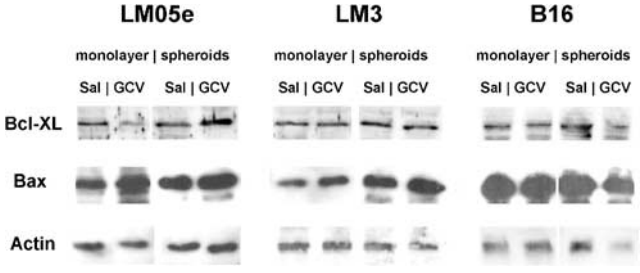

Figure 8 Modulation of Bax and Bcl-XL expression by HSVtk/GCV in monolayers and spheroids. Western blot analysis of Bcl-XL and Bax levels in HSV*tk*-lipofected LM05e, LM3 and B16 monolayers or spheroids treated either with saline (sal) or 10 μg/ml ganciclovir (GCV) performed as described in Materials and methods. Constitutively expressing actin controls are displayed below. Similar results were obtained in three separate experiments.

as GCV treatment proceeded, and we can assume that HSV*tk* expression paralleled this behavior (Fig 6). This effect, and the higher Cx43 expression level (Fig 5), could partially counterbalance the low growing rate of LM05e spheroids (Fig 3), allowing the operation of the HSV*tk*/GCV system. But the possible passage of phosphorylated GCV from one cell to another, cannot explain by itself the successful killing of a high proportion of nonreplicating LM05e spheroid cells, because the GCV mechanism is supposed to absolutely need DNA replication.[3–5] Then, the effectiveness of HSV*tk*/GCV bystander effect may not be restricted to its ability to kill actively dividing cells and supports the involvement of additional cell death mediators.[33–36] Other soluble factor(s) released to extracellular space or small proapoptotic molecules (<1000 Da in size), diffusing from dying cells to their neighbors or transferred trough gap junctions, could be involved in the bystander effect.[33–35] Changes in the intracellular Bax/Bcl-xL apoptosis rheostat could evidence that mitochondria were involved in such an effect.[4,32,33] It has been reported that mitochondria are amplifiers of HSV*tk*/GCV-induced apoptosis, by regulating both the initiation and the effectors phase of apoptosis.[33–35] Mitochondrial free radicals, like highly reactive oxygen free radicals or nitric oxide, could eventually diffuse or pass to adjacent unmodified tumor cells, leading to oxidative damage.[33–35] These events would allow amplification mechanisms where only a few HSV*tk*-expressing cells could destroy the whole spheroid, suggesting the feasibility of the HSV*tk*/GCV approach for some slow growing tumors *in vivo*.

Collectively, all our data suggest that: (i) *in vitro* GCV sensitivity and bystander effect of transiently lipofected cells with *HSVtk* gene is inherent in each individual tumor; (ii) the results obtained in monolayer cultures could not predict the success of this treatment; (iii) monolayer cultures and MCS represent two very different experimental tumor models, therefore (iv) the evaluation of HSV*tk*/GCV treatment may require specific probes on MCS of each tumor system, which represent more closely the *in vivo* situation. On the other hand, the relative resistance of MCS to GCV would depend on: (i) the origin of the tumor cells, (ii) the efficiency of the HSV*tk* transgene transfer and expression; (iii) the diffusion rate of the prodrug through the 3D-structure; (iv) the proliferation state of spheroid cells; (v) gap junction communication; and (vi) changes in the intracellular Bax/Bcl-xL rheostat of mitochondrial-mediated apoptosis.

Further studies on MCS molecular mechanisms and intercellular mediators that could involve sensitivity or resistance toward HSV*tk*/GCV-induced cytotoxicity as (i) GCV active efflux by specific cellular mechanisms (as multidrug resistance) reported as higher in MCS than in monolayer cultures,[36] (ii) transient deprivation of oxygen and/or nutrients, leading to delayed apoptosis,[37] and (iii) development of a form of resistance to killing as the 'contact' effect[38] or the 'good Samaritan effect';[39,40] are imperative to solve this puzzle. Given the low efficiency of currently used gene transfer systems, mechanisms that increase HSV*tk*/GCV sensitivity and bystander effect processes might have important implications to improve the clinical outcome of suicide gene therapy.

Acknowledgments

We thank Gabriela Sobrido and Ana Bihary for technical assistance, Fernanda Roca for histological preparations, and Dr S Klein and Dr M Diament for mice adenocarcinomas. This work was partially supported by a grant from FONCYT: BID802/OC-AR — PICT 05-00037-00709, CABBIO and a grant from BioSidus SA. LMEF, ALK and GCG are members of the Consejo Nacional de Investigaciones Científicas y Técnicas (CONICET, Argentina). VFB and CCC are fellows of CONICET and GLF is a fellow of BioSidus SA.

References

1. Niculescu-Duvaz I, Cooper RG, Stribbling SM, et al. Recent developments in gene-directed enzyme prodrug therapy (GDEPT) for cancer. *Curr Opin Mol Ther*. 1999; 1:480–486.
2. Aghi M, Hochberg F, Breakefield XO. Prodrug activation enzymes in cancer gene therapy. *J Gene Med*. 2000;2: 148–164.
3. Moolten FL. Tumor chemosensitivity conferred by inserted herpes thymidine kinase genes: paradigm for a prospective cancer strategy. *Cancer Res*. 1986;46:5276–5281.
4. Tomicic MT, Thust R, Kaina B. Ganciclovir-induced apoptosis in HSV-1 thymidine kinase expressing cells: critical role of DNA breaks, Bcl-2 decline and caspase-9 activation. *Oncogene*. 2002;21:2141–2153.
5. Pope IM, Poston GJ, Kinsella AR. The role of the bystander effect in suicide gene therapy. *Eur J Cancer*. 1997; 33:1005–1016.
6. Freeman SM, Abboud CN, Whartenby KA, et al. The 'bystander effect': tumor regression when a fraction of the tumor mass is genetically modified. *Cancer Res*. 1993;53:5274–5283.
7. Sutherland RM. Cell and environment interactions in tumor microregions: the multicell spheroid model. *Science*. 1998; 240:177–184.
8. Santini MT, Rainaldi G. Three-dimensional spheroid model in tumor biology. *Pathobiology*. 1999;67:148–157.
9. Mueller-Klieser W. Three-dimensional cell cultures: from molecular mechanisms to clinical applications. *Am J Physiol*. 1997;273:C1109–C1123.
10. Aguirre Ghiso JA, Farias EF, Alonso DF, et al. A phospholipase D and protein kinase C inhibitor blocks the spreading of murine mammary adenocarcinoma cells altering f-actin and beta1-integrin point contact distribution. *Int J Cancer*. 1997;71:881–890.
11. Karara AL, Bumaschny VF, Fiszman GL, et al. Lipofection of early passages of cell cultures derived from murine adenocarcinomas: *in vitro* and *ex vivo* testing of the thymidine kinase/ganciclovir system. *Cancer Gene Ther*. 2001;8:96–99.
12. Urtreger AJ, Diament MJ, Ranuncolo SM, et al. New murine cell line derived from a spontaneous lung tumor induces paraneoplastic syndromes. *Int J Oncol*. 2001;18: 639–647.

13. Frankel A, Buckman R, Kerbel RS. Abrogation of Taxol-induced G_2–M arrest and apoptosis in human ovarian cancer cells grown as multicellular tumor spheroids. *Cancer Res*. 1997;57:2388–2393.
14. Klunder I, Hulser DF. Beta-galactosidase activity in transfected L*tk*− cells is differentially regulated in monolayer and in spheroid cultures. *Exp Cell Res*. 1993;207: 155–162.
15. Kobayashi H, Man S, Kapitain SJ, et al. Acquired multicellular-mediated resistance to alkylating agents in cancer. *Proc Nat Acad Sci USA*. 1993;90:3294–3298.
16. MacGregor GR, Caskey T. Construction of plasmids that express *E. coli* β-galactosidase in mammalian cells. *Nucleic Acids Res*. 1989;17:2365.
17. Felgner JH, Kumar R, Sridhar CN, et al. Enhanced gene delivery and mechanism studies with a novel series of cationic lipid formulations. *J Biol Chem*. 1994;269: 2550–2561.
18. Teifel M, Friedl P. New lipid mixture for efficient lipid-mediated transfection of BHK cells. *Biotechniques*. 1995;19:79–82.
19. Finocchiaro LME, Glikin GC. Intracellular melatonin distribution in cultured cell lines. *J Pineal Res*. 1998;24: 22–34.
20. Dolbeare F, Gray JW. Use of restriction endonucleases and exonuclease III to expose halogenated pyrimidines for immunochemical staining. *Cytometry*. 1988;9:631–635.
21. Bradford MM. A rapid and sensitive method for the quantitation of microgram quantities of protein utilizing the principle of protein-dye binding. *Anal Biochem*. 1976;72:248–254.
22. Yang L, Chiang Y, Lenz HJ, et al. Intercellular communication mediates the bystander effect during herpes simplex thymidine kinase/ganciclovir-based gene therapy of human gastrointestinal tumor cells. *Hum Gene Ther*. 1998;9: 719–728.
23. Hulser DF. Intercellular communication in three-dimensional culture. In: Bjerkvig R, ed *Spheroid Culture in Cancer Research*. Boca Raton, FL: CRC Press; 1992: 172–196.
24. Ballangrud AM, Yang WH, Dnistrian A, et al. Growth and characterization of LNCaP prostate cancer cell spheroids. *Clin Cancer Res*. 1999;5:3171s–3176s.
25. Elion GB, Furman PA, Fyfe JA, et al. Selectivity of action of an antiherpetic agent 9-(2-hydroxyethoxymethyl) guanine. *Proc Natl Acad Sci USA*. 1977;74:5716–5720.
26. Elion GB. The chemotherapeutic exploitation of virus-specified enzymes. *Adv Enzyme Regul*. 1980;18:53–60.
27. Touraine RL, Ishii-Morita H, Ramsey WJ, Blaese RM. The bystander effect in the HSV*tk*/ganciclovir system and its relationship to gap junctional communication. *Gene Therapy*. 1998;5:1705–1711.
28. Namba H, Iwadate Y, Kawamura K, et al. Efficacy of the bystander effect in the herpes simplex virus thymidine kinase-mediated gene therapy is influenced by the expression of connexin43 in the target cells. *Cancer Gene Ther*. 2001;8:414–420.
29. King TJ, Fukushima LH, Hieber AD, et al. Reduced levels of connexin43 in cervical dysplasia: inducible expression in a cervical carcinoma cell line decreases neoplastic potential with implications for tumor progression. *Carcinogenesis*. 2000;6:1097–1109.
30. Cirenei N, Colombo BM, Mesnil M, et al. *In vitro* and *in vivo* effects of retrovirus-mediated transfer of the connexin 43 gene in malignant gliomas: consequences for HSV*tk*/GCV anticancer gene therapy. *Gene Therapy*. 1998;5: 1221–1226.
31. Knuechel R, Siebert-Wellnhofer A, Traub O, et al. Connexin expression and intercellular communication in two- and three-dimensional *in vitro* cultures of human bladder carcinoma. *Am J Pathol*. 1996;149:1321–1332.
32. Craperi D, Vicat JM, Nissou MF, et al. Increased bax expression is associated with cell death induced by ganciclovir in a herpes thymidine kinase gene-expressing glioma cell line. *Hum Gene Ther*. 1999;10:679–688.
33. Beltinger C, Fulda S, Kammertoens T, et al. Mitochondrial amplification of death signals determines thymidine kinase/ganciclovir-triggered activation of apoptosis. *Cancer Res*. 2000;60:3212–3217.
34. Herdener M, Heigold S, Saran M, Bauer G. Target cell-derived superoxide anions cause efficiency and selectivity of intercellular induction of apoptosis. *Free Radic Biol Med*. 2000;29:1260–1271.
35. Bi WL, Parysek LM, Warnick R, Stambrook PJ. *In vitro* evidence that metabolic co-operation is responsible for the bystander effect observed with HSV*tk* retroviral gene therapy. *Hum Gene Ther*. 1993;4:725–731.
36. Kolchinsky A, Roninson IB. Drug resistance conferred by MDR-1 expression in spheroids formed by glioblastoma cell lines. *Anticancer Res*. 1997;17:3321–3328.
37. Jacobson MD, Raff MC. Programmed cell death and bcl-2 protection by very low oxygen. *Nature*. 1995;374:814–816.
38. Luo C, MacPhail SH, Dougherty GJ, et al. Radiation response of connexin 43-transfected cells in relation to the 'contact effect'. *Exp Cell Res*. 1997;234:225–232.
39. Wygoda MR, Wilson MR, Davis MA, et al. Protection of the herpes simplex virus thymidine kinase-transduced cells from ganciclovir-mediated cytotoxicity by bystander cells: the Good Samaritan effect. *Cancer Res*. 1997;57: 1699–1703.
40. Andrade-Rozental AF, Rozental R, Hopperstad MG, et al. Gap junctions: the 'kiss of death' and the 'kiss of life'. *Brain Res Rev*. 2000;32:308–315.